Use of Proton SEE Data as a Proxy for Bounding Heavy-Ion SEE Susceptibility

Ray Ladbury[1] and Jean-Marie Lauenstein[1] and Kathryn P. Hayes[2]

[1]NASA -GSFC code 561.4, Greenbelt, MD 20771.   [2]Vanderbilt University, Nashville, TN 37203

Abstract: We examine use of proton SEE data to constrain heavy-ion SEE susceptibility. We discuss limitations due to short range proton recoils and develop an approach for using proton data to constrain device sensitive volumes.

Introduction, Data and Method

Although heavy-ion single-event effects (SEE) pose serious threats to semiconductor devices in space, many missions face difficulties testing such devices at heavy-ion accelerators. Low-cost missions often find such testing too costly. Even well funded missions face issues testing commercial off the shelf (COTS) parts due to packaging and integration.[1,2] Some missions wish to fly COTS systems without investigating their performance component by component. Heavy-ion testing such parts and systems requires expensive and hard-to-access ultra-high energy ion accelerators,[3] or significant system modification. To avoid these problems, some have proposed using recoil ions from high-energy protons as a proxy to bound heavy-ion SEE rates.[4-7]

While proton testing avoids the range issues of heavy-ion testing (see fig. 1), potentially producing ions (in pure Si) with linear energy transfer (LET) up to 15 MeVcm2/mg, bounding heavy-ion SEE with proton testing is also challenging (see fig. 2). This is particularly true for destructive SEE.[8-11]
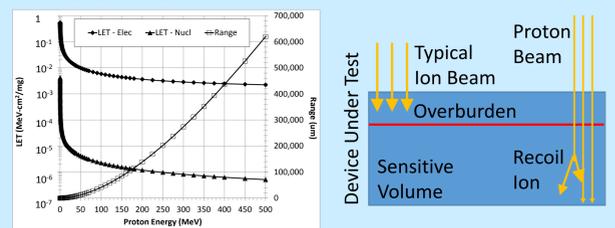

Fig.1 Heavy ions from accelerators impinge on devices under test (DUT) with a uniform energy and angle, so that if there is too much overburden, they range out before reaching the sensitive volume. Protons have much greater range. Although most protons lose energy slowly, a few interact strongly with nuclei in the lattice, generating ion recoils, which emerge with a range of energies, angles and even ion species.

The difficulty of bounding heavy-ion SEE rates with proton SEE data arises from the complex kinematics of proton-nuclear recoils. While [4-7] consider recoil ion production vs. ion species, energy and angle, the emphasis is on the Linear Energy Transfer (LET) spectrum of recoils. The authors conclude that irradiation with 10^{10} protons/cm2 equates to heavy-ion testing up to LET > 8 MeVcm2/mg.

However, describing space heavy ions in terms of LET oversimplifies the situation. For small (<<1 μm3) SV, LET describes average energy loss, while SEE may result from rare events (energetic delta rays) that represent fluctuations away from the average indicated by LET.[12] Extreme events for high-energy ions deposit far more energy in a small SV than events of similar probability for low-energy ions. In large SV, LET varies along the ion path, especially for low-energy ions. Over 99% of recoils with atomic number Z>8 are on the low-energy side of the Bragg Peak.
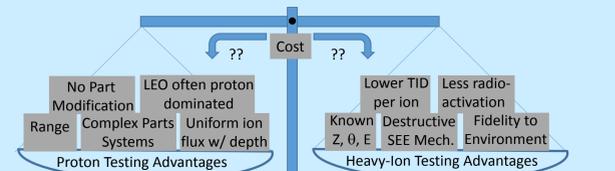

Fig. 2 Whether testing with heavy ions or protons is the preferred strategy depends on a variety of factors ranging from ion kinematics to part susceptibilities to questions of feasibility.

We use the CRÈME-MC physics based Monte Carlo package[13,14] on the Vanderbilt University Cluster to generate proton recoils and measure the energy they deposited in the SV of various dimensions characteristic of destructive and nondestructive SEE. CRÈME-MC uses the Monte Carlo Radiative Energy Deposition (MRED) package, which in turn uses the GEM03 nuclear code for proton-nuclear interactions. These codes have been validated extensively and found to be in good agreement with empirically measured cross sections.[15]

Destructive SEE Mechanisms

Destructive SEE (DSEE) are among the most serious threats facing many missions. They are also difficult to bound with proton data, since DSEE susceptibility often depends on more than ion LET. See Figs. 3-4.
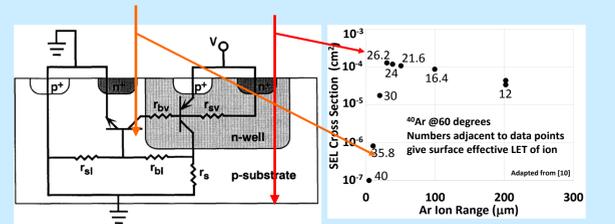

Fig.3 Since SEL is a parasitic bipolar phenomenon that inherently involves the substrate, the SEL SV often extends several 10s of μm into the substrate. [10] found that for cryogenic SEL at 20 K, short-range ions yielded cross sections >1000x lower than ions depositing a maximum energy in the SV, and that increasing ion range increased cross section up to a range of 35 microns. [11] noted similar effects for conventional (room temperature) SEL. Thus, using proton data will significantly underestimate the heavy-ion SEL susceptibility if it looks at ion LET rather than charge deposited by the ion.
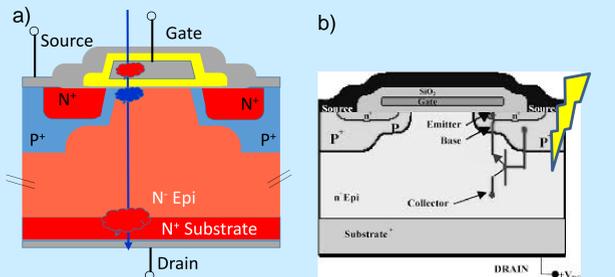

Fig. 4 a) SEGR depends not just on ion LET or charge deposited in the SV, but also on ion angle of incidence and atomic number Z. The angular and Z dependencies (likely the result of momentary gate oxide weakening by the ion), limit the number of proton recoils that can cause SEGR. Similar effects occur in FLASH memory[16] and some bipolar technologies.[17]. b) Like SEL, SEB is a parasitic bipolar effect. While ion range is usually less critical than for SEL and SEGR, [9] shows SEB voltage decreasing for short range ions (<30 μm). This work also suggests SEB vulnerability may increase with Z. These factors, along with the angular dependence suggest proton recoils will likely underestimate SEB vulnerability significantly.

Representative Sensitive Volumes

While DSEE SV have complicated geometries, simplified SV suffice to illustrate the difficulties of using proton data as a proxy for bounding heavy-ion SEE rates. We represented the SV as cubes surrounded by inert Si. (See fig. 5). The smallest SV was a 1 μm cube, roughly representative of charge collection volumes for nondestructive SEE. Although SV for deep submicron are smaller, we wanted to avoid situations where ions fluctuated significantly away from constant-LET behavior over short distances. The largest SV was a 10 μm cube. This is a fairly shallow charge collection depth z for DSEE. However, it demonstrates the problems arising from using proton recoils as a proxy for heavy-ion test data, and for any deeper SV, protons recoils would only deviate further accelerator or galactic cosmic ray (GCR) heavy ions. We defined an equivalent LET as the average energy deposited (E_{Dep}) in the SV normalized to the material density ρ:

$$LET_{EQ} = \frac{E_{Dep}}{(\rho \times z)}$$

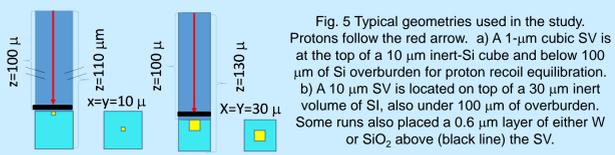An ion with this constant LET would deposit the same charge in the SV.

Fig. 5 Typical geometries used in the study. Protons follow the red arrow. a) A 1-μm cubic SV is at the top of a 10 μm inert-Si cube and below 100 μm of Si overburden for proton recoil equilibration. b) A 10 μm SV is located on top of a 30 μm inert volume of SI, also under 100 μm of overburden. Some runs also placed a 0.6 μm layer of either W or SiO2 above (black line) the SV.

Results and Discussion

Figs. 6-7 illustrate the dependence of LET_{EQ} on proton fluence and the size of the sensitive volume. Regardless of the SV size, LET_{EQ} increases rapidly for proton energies (E_p) 20-50 MeV, but flattens out for E_p from 100-500 MeV. Plots were generated assuming a saturated heavy-ion saturated cross section σsat of 10^{-4} cm2.
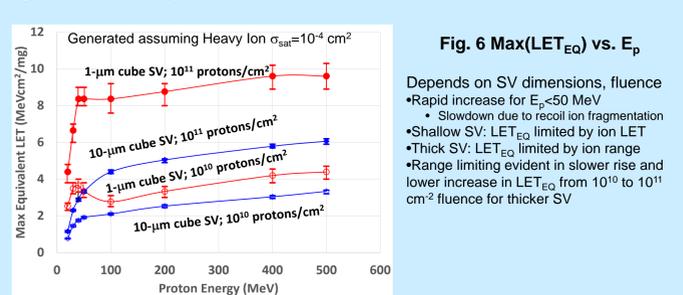

Fig. 6 Max(LET_EQ) vs. E_p

Depends on SV dimensions, fluence
• Rapid increase for E_p<50 MeV
  • Slowdown due to recoil ion fragmentation
• Shallow SV: LET_{EQ} limited by ion LET
• Thick SV: LET_{EQ} limited by ion range
• Range limiting evident in slower rise and lower increase in LET_{EQ} from 10^{10} to 10^{11} cm-2 fluence for thicker SV
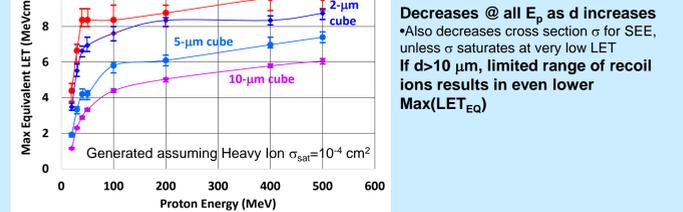

Fig. 7 Max(LET_EQ) vs. SV depth, d

Decreases @ all E_p as d increases
• Also decreases cross section σ for SEE, unless σ saturates at very low LET
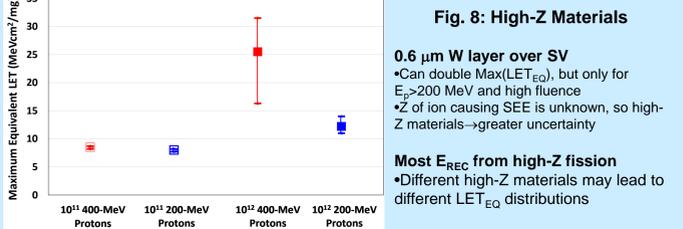If d>10 μm, limited range of recoil ions results in even lower Max(LET_{EQ})

Fig. 8 shows how high-Z material can significantly increase the maximum LET_{EQ} in the SV. The fission of the high-Z ion imparts significant energy E_{REC} to recoil ion(s).

Fig. 8: High-Z Materials

0.6 μm W layer over SV
• Can double Max(LET_{EQ}), but only for E_p>200 MeV and high fluence
• Z of ion causing SEE is unknown, so high-Z materials →greater uncertainty

Most E_{REC} from high-Z fission
• Different high-Z materials may lead to different LET_{EQ} distributions

The fact that the LET_{EQ} from this study are consistent with the LET found in [4-6] for shallow SV, but are significantly lower for deep SV suggests that the limited range of proton recoils is responsible for the differences rather than any differences in the physics models. To verify this, we combined differential energy cross section (figure 3 from [6]) with ion species production (figure 7 from [6]). The results in Fig. 9 suggest few proton recoils have energy higher than the Bragg peak. The chances of one of these traversing a long chord length in a deep SV are small.
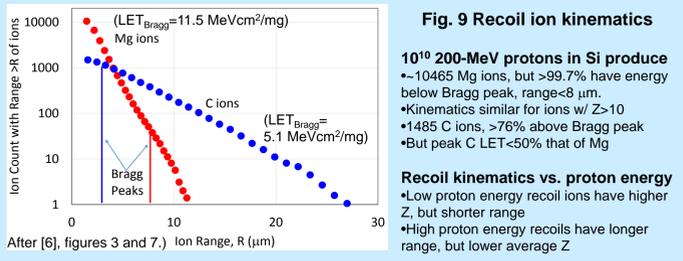

Fig 9 Recoil ion kinematics

(LET_{Bragg}=11.5 MeVcm2/mg) Mg ions

10^{10} 200-MeV protons in Si produce
• ~10465 Mg ions, but >99.7% have energy below Bragg peak, range<8 μm.
• Kinematics similar for ions w/ Z>10
• 1485 C ions, >76% above Bragg peak
• But peak C LET<50% that of Mg

(LET_{Bragg}= 5.1 MeVcm2/mg) C ions

Recoil kinematics vs. proton energy
• Low proton energy recoil ions have higher Z, but shorter range
• High proton energy recoils have longer range, but lower average Z

After [6], figures 3 and 7.)

Hardness Assurance Implications

The discussion of DSEE mechanisms and the Monte Carlo results paint a pessimistic picture for use of proton data to bound heavy-ion DSEE rates. The Z, angular and range dependence of SEGR and SEB suggest proton testing will significantly underestimate SEB/SEGR risk if it detects the susceptibility at all.

The situation is more favorable for SEL. However, improperly accounting for SV depth d can underestimate the SEL rate by >20x (for d=10 μm) for proton test fluences of 10^{10} 200-MeV protons/cm2 or >5x if the fluence is 10^{11} cm-2. If the charge collection depth is deeper (common for SEL), the underestimate will be even worse. Moreover, since SEL cross section scales with collected charge (and therefore LET_{EQ}), the area vulnerable to proton-induced SEL may be significantly smaller than would be assuming it scaled with LET.

For nondestructive SEE, charge collection volumes are shallower, and our results of would likely match those of [4-7] for SV sufficiently large that the constant LET assumption is valid. However, [12] showed that the broader charge-track distribution for high-energy ions can trigger error modes that would not be revealed by low-energy proton recoils. At the 22 nm node and below, this could be a significant concern for multi-bit upsets and upsets in hardened latches that rely on spatially separated redundant nodes for their hardening.

Generalized Linear Model

Although proton SEE test data can constrain heavy-ion SEE susceptibility, bounding destructive SEE modes remains problematic. The previous discussion has shown that the only DSEE mode where proton testing might provide useful bounds is SEL—and even then, a single-energy irradiation may not provide sufficient information about the SEL SV to bound the failure rate. Even for nondestructive SEE, a single-energy test is unlikely to place meaningful bounds on susceptibility in any but the most benign heavy-ion environments. This raises the question of whether multiple energies might be combined to improve the bounds. Low-energy proton recoils tend to produce short-range recoils with 10≤Z≤14, while high-energy proton recoils prodce comparable ion counts with Z>8 and Z>10, but have longer ranges. The result of these differences can be seen in Fig. 8, where LET_{EQ} saturates at lower energy for shallow SV than for deeper SV. Thus, use of multiple proton energies could differentiate between candidate SV and better constrain SEE rates.

We assumed a Weibull form for the heavy-ion cross section vs. LET and constrained the Weibull parameters with a Generalized Linear Model as in [18]. (See Figure 10.) Due to the short proton recoil range, we parameterize the Weibull in LET_{EQ} rather than LET and generated proton recoil LET_{EQ} distributions $\phi(LET_{EQ},E_p,d,\sigma)$ for various candidate SV. When stored as a look-up table, these distributions serve as a CRÈME-MC emulator to determine which candidate SV are consistent with proton data.

$N(E_p)$=Observed SEE vs E_p

$\phi(LET_{EQ},E_p,d,\sigma)$ Look-up Tables for CRÈME-MC Emulator

Generalized Linear Model

$$\mu(E_p,d) = \int_0^{MAX(LET_{EQ})} N_{cv}\phi(LET_{EQ},E_p,d,\sigma(LET_{EQ})) \times \sigma(LET_{EQ}) dLET_{EQ}$$

$$L(d,\sigma_{lim},LET_0,w,s) = \prod_i Poisson[N(E_p),\mu(E_p,d,\sigma_{lim},LET_0,w,s)]$$

$$\sigma(LET_{EQ}) = \sigma_{lim} \times (LET_{EQ} - LET_0,w,s)$$

Select σ_{lim}, LET_0, w, s, and d consistent with desired confidence and yielding WC rate

Fig. 10 Generalized Linear Model for constraining heavy-ion SEE data with proton SEE data for multiple proton energies, E_p.

Conclusions

We have examined the effect on device SV geometry on the conclusions that can be drawn from proton SEE data for heavy-ion SEE susceptibility. We find that for devise SV with depths greater than about 5 microns, charge generation by recoil ions from proton-ion collisions tends to be limited by the ion's range rather than its LET. This means that proton data place very weak constraints on heavy-ion induced SEL. Similar considerations apply for SEGR and SEB. However, dependence on ion angle of incidence and ion species for these failure modes mean that generalizing from proton data to heavy-ion susceptibility is risky.

We also propose a generalized linear model approach for using proton SEE data to bound heavy-ion SEE susceptibilities that allows data for several proton energies to be combined to draw more reliable conclusions about device SV geometries from proton data.

Acknowledgment

References

[1]   R. Ladbury, et al. "Radiation Performance of 1 Gbit DDR2 SDRAMs Fabricated with 80-90 nm CMOS," IEEE Radiation Effects Data Workshop 2008, p. 42, 2008.

[2]   P. M. Gouker, et al, "Radiation Effects in 3D Integrated SOI SRAM Circuits," IEEE Trans. Nucl. Sci., Vol. 58, No. 6, p. 2845, 2011.

[3]   S. Buchner, et al., "Variable Depth Bragg Peak Method for Single Event Effects Testing," IEEE Trans. Nucl. Sci., Vol. 58, No. 6, p. 2976, 2011.

[4]   P. O'Neill, G. Badhwar, and W. Culpepper, "Risk Assessment for Heavy Ions of Parts Tested with Protons," IEEE Trans. Nucl. Sci., Vol. 44, No. 6, p. 2311, 1997.

[5]   P. O'Neill, G. Badhwar, and W. Culpepper, "Internuclear cascade-evaporation model for LET spectra of 200 MeV protons used for parts testing," IEEE Trans. Nucl. Sci., vol. 45, pp. 2467–2474, Dec. 1998.

[6]   D. M. Hiemstra and E. W. Blackmore, "LET Spectra of Proton Energy Levels From 50 to 500 MeV and Their Effectiveness for Single Event Effects Characterization of Microelectronics," IEEE Trans. Nucl. Sci., Vol. 50, NO. 6, page 2245, 2003.

[7]   J. Barak, "Analytical Microdosimetry Model for Proton-Induced SEU in Modern Devices," IEEE Trans. Nucl. Sci., Vol. 48, NO. 6, page 1937, 2001.

[8]   J.-M. Lauenstein, et al., "Effects of Ion Atomic Number on Single-Event Gate Rupture (SEGR) Susceptibility of Power MOSFETs," IEEE Trans. Nucl. Sci., Vol. 58, No. 6, p. 2628, 2011.

[9]   S. Liu et al., "Effects of Ion Species on SEB Failure Voltage of Power DMOSFET," IEEE Trans. Nucl. Sci., Vol. 58, No. 6, p. 2991, 2011.

[10]   C. J. Marshall, "Mechanisms and Temperature Dependence of Single Event Latchup Observed in a CMOS Readout Integrated Circuit From 16–300 K," IEEE Trans. Nucl. Sci., Vol. 57, No. 6, p. 3078, 2010.

[11]   A. H. Johnston and B. W. Hughlock, "LATCHUP IN CMOS FROM SINGLE PARTICLES," IEEE Trans. Nucl. Sci., vol. 37, No. 6, p. 1886, 1996.

[12]   A. H. Johnston, "The influence of VLSI technology evolution on radiation-induced latchup in space systems," IEEE Trans. Nucl. Sci., vol. 43, No. 6, p. 505, 1996.

[13]   M. P. King, et al. "The Impact of Delta-Rays on Single-Event Upsets in Highly Scaled SOI SRAMs," IEEE Trans. Nucl. Sci., Vol. 57, NO. 6, page 3169, 2010.

[14]   R.A. Weller, et al., "Monte carlo simulation of single event effects," IEEE Trans. Nucl. Sci., vol. 57, no. 4, p. 1726, Aug. 2010.

[15]   J. H. Adams, et al., "CRÈME: The 2011 Revision of the Cosmic Ray Effects on Micro-Electronics Code," IEEE Trans. Nucl. Sci., Vol. 59, No. 6, p. 3141, 2012.

[16]   M. S. Sabra, "Validation of Nuclear Reaction Codes for Proton-Induced Radiation Effects: The Case for CEM03," IEEE Trans. Nucl. Sci., Vol. 58, No. 6, p. 3134, 2011.

[17]   T. R. Oldham, D. Chen, S. P. Buchner, and K. A. Label, "Radiation Effects Test Guideline Document for Nonvolatile Memories: Lessons Learned," https://nepp.nasa.gov/files/24671/Oldham_2013_NVM_Guideline.pdf, 5/31/2015

[18]   G. K. Lum, H. O'Donnell, and N. Boruta, "The impact of single event gate rupture in linear devices," IEEE Trans. Nucl. Sci., vol. 47, p. 2373–2379, Dec. 2000.

[19]   R. Ladbury, "Statistical Properties of SEE Rate Calculation in the Limits of Large and Small Event Counts," IEEE Trans. Nucl. Sci., Vol. 54, No. 6, p. 2113, 2007.